Published online 27 March 2007

Nucleic Acids Research, 2007, Vol. 35, No. 7 ***2321–2332***
doi:10.1093/nar/gkm127

Conserved interactions of the splicing factor Ntr1/Spp382 with proteins involved in DNA double-strand break repair and telomere metabolism

Gernot Herrmann[1,*], Sanja Kais[2], Jan Hoffbauer[1], Kijwasch Shah-Hosseini[1], Nicole Brüggenolte[1], Heiko Schober[4], Margaret Fäsi[3] and Primo Schär[2]

[1]Department of Dermatology, University of Cologne, D-50924 Cologne, Germany, [2]Centre for Biomedicine, University of Basel, CH-4058 Basel, Switzerland, [3]Institute of Molecular Cancer Research, University of Zürich, CH-8008 Zürich, Switzerland and [4]Friedrich Miescher Institute for Biomedical Research, CH-4058 Basel, Switzerland

Received November 22, 2006; Revised February 14, 2007; Accepted February 15, 2007

ABSTRACT

The ligation of DNA double-strand breaks in the process of non-homologous end-joining (NHEJ) is accomplished by a heterodimeric enzyme complex consisting of DNA ligase IV and an associated non-catalytic factor. This DNA ligase also accounts for the fatal joining of unprotected telomere ends. Hence, its activity must be tightly controlled. Here, we describe interactions of the DNA ligase IV-associated proteins Lif1p and XRCC4 of yeast and human with the putatively orthologous G-patch proteins Ntr1p/Spp382p and NTR1/TFIP11 that have recently been implicated in mRNA splicing. These conserved interactions occupy the DNA ligase IV-binding sites of Lif1p and XRCC4, thus preventing the formation of an active enzyme complex. Consistently, an excess of Ntr1p in yeast reduces NHEJ efficiency in a plasmid ligation assay as well as in a chromosomal double-strand break repair (DSBR) assay. Both yeast and human NTR1 also interact with PinX1, another G-patch protein that has dual functions in the regulation of telomerase activity and telomere stability, and in RNA processing. Like PinX1, NTR1 localizes to telomeres and associates with nucleoli in yeast and human cells, suggesting a function in localized control of DSBR.

INTRODUCTION

Double-strand breaks (DSBs) can arise in DNA through genotoxic stress or as a consequence of DNA metabolic processes associated with DNA synthesis and cell differentiation. Such breaks are highly cytotoxic and will kill a cell, unless repaired. Inaccurate repair, however, will lead to the loss or alteration of genetic information, promoting tumorigenesis and aging. Nature has evolved two fundamentally different strategies for DSB repair (DSBR); homologous recombination (HR) and non-homologous end-joining (NHEJ). Although their relative biological significance varies across the phylogeny, HR and NHEJ are highly conserved repair systems that require a high level of coordination if genomic instability by misrepair is to be avoided (1,2).

NHEJ in mammalian and yeast cells requires a set of common core factors, including the DNA end-binding proteins Ku70 (Ku70p) and Ku80 (Ku80p), as well as the DNA ligase LIG4 (Dnl4p) and its associated factor XRCC4 (Lif1p) (3–6). Yeast Lif1p is detectable near DNA ends, suggesting that it binds DNA in cooperation with Ku and targets Dnl4p to the DSB (7). Similarly, Ku proteins together with the p460 kinase subunit of DNA-PK_{cs} are necessary to recruit the XRCC4-LIG4 complex to DNA ends in human cells (8). Additional factors that contribute to the synapsis and processing of double-stranded DNA ends, including the DNA-PK_{cs}, the MRE11/RAD50/NBS1 (Xrs2p) complex, or Artemis appear to be less conserved between single and multi-cellular organisms [e.g.(9,10)]. Several key components of the NHEJ pathway, e.g. Ku70/80, MRE11/RAD50/NBS1 and Sir proteins, associate with telomeres in lower and higher eukaryotes where they contribute to telomeric maintenance. Telomeres, the free ends of eukaryotic chromosomes, form specialized structures that distinguish them from internal chromosomal breaks and prevent undesired ligation by the NHEJ pathway (11,12).

With an objective to identify regulatory components of the NHEJ pathway, we set out to isolate proteins interacting with Lif1p in a two-hybrid screen in *Saccharomyces cerevisiae*. We isolated two interacting proteins. One of them, Nej1p, was then shown to be a

*To whom correspondence should be addressed. Tel: +49-221-478-7341; Fax: +49-221-478-5949; Email: gernot.herrmann@uni-koeln.de

cell-type-specific regulator of NHEJ in yeast (13–16). The majority of positive clones, however, contained a fragment of an open reading frame (ORF), denoted as YLR424W in the *S. cerevisiae* genome database. YLR424W encodes Ntr1p (Nineteen complex-related protein; standard name SPP382 at SGD), an essential protein with a G-patch domain, which was recently described as a factor involved in spliceosome disassembly (17–19). G-patches are short conserved sequences of ~40 amino acids containing seven highly conserved glycine residues that have been proposed to mediate RNA binding (20). G-patches have also been found in tumor suppressors and DNA-repair proteins (21–25). We show here that Ntr1p associates with Lif1p in a way that excludes binding of Dnl4p and, doing so, forms a stable ternary complex with Lif1p and Nej1p. An *ntr1*Δ disruption causes lethality, but overexpression in yeast affects NHEJ in a plasmid ligation assay and DSBR in a chromosomal context. Ntr1p and its interaction with Lif1p is conserved as we show that a human putative NTR1 ortholog, known as TFIP11 (tuftelin interacting protein), competes with LIG4 for the binding to XRCC4. Like the yeast counterpart, the human NTR1 has been implicated in RNA splicing (26,27). Both the yeast and the human NTR1 proteins further interact with the respective orthologs of PinX1 (PinX1p), another G-patch-containing protein. PinX1 localizes to the nucleolus and to telomeres and appears to have dual functions in RNA processing and the modulation of telomerase activity (22,28). Yeast and human NTR1 also appear to localize to telomeres and to nucleoli. Thus, our data suggest that yeast and human NTR1 are members of a newly emerging family of G-patch proteins that have multiple functions in RNA splicing, DNA repair and telomere maintenance, including also PinX1 (22,28–30), and the orthologs TgDRE of *Toxoplasma gondii* (23,24), DRT111 of *Arabidopsis thaliana* (21) or SPF45 of *Drosophila melanogaster* (25).

MATERIALS AND METHODS

Yeast strains and growth conditions

Saccharomyces cerevisiae strains FF18734, FF18984, FF18743 (*rad52*Δ) and PRSY003,1 (*dnl4*Δ) used in this study are isogenic derivatives of two closely related, congenic series in an A364A background (4). Yeast strains AH109 and Y187 (Clontech) were used for two- and three-hybrid analysis. The *ntr1*Δ deletion was a precise deletion of the ORF, marked by KAN-MX4 (Research Genetics). Cells were grown at 30°C in yeast complete medium or appropriate synthetic drop out media.

Plasmids, DNA manipulations and sequence analyses

For two-hybrid analysis, different fragments of *LIF1*, *DNL4* or human *LIG4* were PCR-amplified from pGEH019, pGEH009 or pGEH007, respectively (3) and subcloned into the Gal4-BD vector pAS2-1, or Gal4-AD vector pACT2 (BD Clontech). The entire *S. cerevisiae NTR1* or *PINX1* ORFs were amplified by PCR of genomic DNA from FF18743 and subcloned into pACT2 or pAS2-1 (BD Clontech). XRCC4 was PCR-amplified from a construct containing the entire ORF (31). Plasmids containing the full-length ORF of human NTR1 were obtained from DKFZ, Heidelberg, Germany (DKFZp434B194, Accession No. AL080147); PinX1 (MGC-8850) and TRF1 (3118244) cDNAs were from ATCC. All plasmids containing entire ORFs were then used as templates for further PCR amplification of fragments which were then cloned into appropriate yeast or bacterial expression vectors. For co-expression studies in bacteria and yeast, we used the IPTG-inducible expression vector pET-28(c) (Novagen) or pGEX-KG. For co-expression studies in yeast, we used the galactose-inducible expression vector pYes2 (Invitrogen). *LIF1* was co-expressed in yeast from pGEH014 (3). yEGFP-sc*NTR1* and yEGFP-hu*NTR1* were constructed by fusing the full-length *NTR1* genes to the MET25 promoter and yEGFP sequences in plasmid pUG36 (16). For transient expression in human cells, fragments of human NTR1 were fused to ECFP, and were then PCR-amplified and subcloned into the tetracycline-inducible vector pcDNA4/TO/*myc*-His (Invitrogen). TRF1 was fused with red fluorescent protein in pDsRed2-C1 or with green fluorescent protein in pDsGreenC1 (Clontech). All constructs were verified by sequencing using an ABI 377 DNA sequencer (Perkin Elmer). Primer sequences and details are available on request. For general database searches and comparisons, we used the BLAST, FASTA and ENTREZ services provided at NCBI's web page; for yeast genome database searches, we accessed MIPS and SGD through their web pages.

Two-hybrid and three-hybrid analysis

Two-hybrid screening was performed using the Matchmaker™ two-hybrid system from Clontech. A *S. cerevisiae* two-hybrid library was kindly provided by Dr N. Lowndes, Galway, Ireland. A pretransformed Human HeLa Matchmaker™ cDNA Library was obtained from Clontech. Three-hybrid analysis was carried out according to the manufacturer's recommendations (Clontech). In extension to two-hybrid analysis, three-hybrid analysis allows investigation of ternary protein complex formation by expression of a third protein cloned into vector pBridge (Clontech) under the control of a methionine-repressible promotor (32). Expression was induced by omitting methionine from the growth medium of the yeast cells. β-Galactosidase assays were carried out according to standard protocols (33).

NHEJ and chromosomal breakage assays

Ligation of restriction endonuclease-digested linearized plasmids and chromosomal breakage assays were carried out as described previously (4,34). Briefly, yeast strains were co-transformed with plasmids carrying the URA3 marker gene and either expressing HO, or EcoRI endonuclease (35) under the control of the inducible *GAL1* promoter and the plasmid-expressing NTR1. Four individual URA+ transformants of each strain were grown to late exponential phase (5×10^7 cells/ml) in liquid medium lacking uracil at 30°C before dropping 5 µl

of serial dilutions (2×10^7, 2×10^6, 2×10^5, 2×10^4, 2×10^3 cells/ml) onto media containing 2% of either glucose, raffinose or raffinose + galactose. The plates were incubated at 30°C for 3–5 days and then photographed. For quantitative analyses, c.f.u. of appropriate dilutions were counted and percentages of survival calculated from at least three independent experiments.

Protein purification and western blot analysis

Purification of 6× histidine-tagged Lif1p from *E. coli* and of 6× histidine-fused proteins from *S. cerevisiae* was performed as described elsewhere (3). GST-tagged fragments of human and yeast NTR1, or PinX1 were expressed alone or co-expressed in different combinations with Lif1p, XRCC4 or NTR1 [in pET28(c)], and purified from *E. coli* BL21(DE3) cells using glutathione sepharose beads. 6× histidine-fused yeast or human NTR1 were co-expressed with Lif1p in yeast strain FF18734 and purified as described elsewhere (3). Induction with galactose (2%) was performed for 10 h. To minimize unspecific binding to the corresponding columns and to increase stringency, washes were performed in a buffer that contained 637 mM NaCl, 2.7 mM KCl, 10 mM phosphate, 0.2% NP-40, 1 mM β-mercaptoethanol; pH 7.4. HeLa and WI26 VA4 cell extracts were prepared with RIPA buffer (supplemented with 4 mM EDTA, 0.2% *n*-dodecyl-β-maltoside, protease inhibitors and ethidium bromide) and 5 mg of extracts were incubated with glutathione sepharose-bound GST-fusion proteins or glutathione sepharose beads overnight at 4°C. Western blot analysis was carried out as described elsewhere (3). Affinity-purified anti-LIF1 antibody was used at a dilution of 1:1000 in PBS containing 1% (w/v) non-fat dried milk, 0.1% Tween-20 for 1 h at room temperature; anti-scNtr1p and anti-huNTR1 antibodies were used at dilutions of 1:200 and 1:2000, respectively, in the same buffer (details on antibody generation on request); anti-XRCC4 (ab2857, Abcam), anti-6× histidine (Cell Signaling) and anti-GFP antibodies (11E5 Invitrogen) were used at dilutions of 1:1000. Anti-PinX1 (ab2344, Abcam) was used at 1:100 overnight at 4°C. Secondary antibodies conjugated to horseradish peroxidase (Pierce, Rockford) were used at dilutions of 1:2000–1:7500.

Microscopic analyses of yeast and human cells

The interaction between Ntr1p and telomeric protein Rap1p was investigated following transformation of the FF18734 strain with plasmid constructs expressing EGFP-NTR1 under the control of the inducible Met25 promoter. Cells were incubated overnight in the liquid minimal medium supplemented with methionine to the final concentration of 1 mM. Cells were prepared for immunofluorescence according to a protocol described previously (36). The endogenous Rap1p was detected using rabbit polyclonal antibody (gift from Susan Gasser) diluted 1:200 in PBS and goat anti-rabbit-TRITC (Sigma) diluted 1:50 in PBS. The signals from EGFP and TRITC were visualized on the confocal Zeiss LSM 510 META microscope with ×63 Plan-Apochromat objective (1.4 oil). An argon laser at 488 nm was used to detect EGFP fluorochrome. To detect TRITC fluorochrome, a helium–neon laser was filtered at 543 nm, while for the DAPI fluorochrome a laser diode was filtered at 405 nm. For image capture, standardized conditions for the pinhole size, gain and offset were used. Each image is an average of eight scans. Images were deconvolved using the Huygens program. To visualize co-localization between Ntr1p and nucleolar protein Nop1, the FF18734 strain was co-transformed with plasmids pUG36-EGFP-NTR1 and pGVH45 (carrying NOP1-CFP; gift from Susan Gasser). The cells were grown overnight in liquid medium (to select for the both plasmids) supplemented with methionine to the final concentration of 1 mM (to keep the levels of EGFP-Ntr1p low). For the live cell imaging, cells were spread on SC agar patches containing 4% glucose. The Metamorph-driven Olympus IX70 microscope equipped with a Zeiss 100×/1.4 oil objective was used to capture 21 image stacks of 200-nm step size (two sequential wavelength 432/515 nm, Chromas filter cube CFP/YFP). The image stacks were deconvolved using the Metamorph program.

Transfections of human WI26 VA4 fibroblasts were performed with FuGENE^{TM} (Boehringer Mannheim) and the Tet-On expression system (BD Biosciences) according to the manufacturer's instructions. Tetracycline induction of ECFP-NTR1 was performed for 4 at 16 h after transfection. Cells were formaldehyde-fixed (3.7%, 15 min at room temperature). Confocal images were taken with an inverted Leica TCS-SP laser-scanning microscope with a ×3 PL Fluotar 1.32–0.6 oil immersion objective. The 488-nm argon ion laser line was used for excitation of ECFP and the 588-nm krypton ion laser line for DsRed2. DAPI was excited using a two-photon laser (772 nm, Spectra Physics). Under all imaging conditions used, no signal from one fluorochrome could be detected on the other filter set. Images were processed using the accompanying software. All images were prepared for publication using Adobe Photoshop.

RESULTS

Ntr1p interacts with Lif1p

We set out to identify interaction partners of the DNA ligase IV-associated protein Lif1p by two-hybrid screening of a yeast cDNA library. Full-length Lif1p and a C-terminal deletion variant consisting of the first 260 amino acids only served as baits. We isolated several clones containing parts of the ORF YLR424W that locates on chromosome XII. YLR424W encodes an 83-kDA protein of 708 amino acids that was recently described as a factor involved in spliceosome disassembly, Ntr1p (17–19). Two-hybrid-based mapping of the Ntr1p interaction site in Lif1p revealed that amino acids between 220 and 240 are essential for interaction (Figure 1A and B). This is the region also required for efficient interaction with Dnl4p (Figure 1B) (3), and where Lif1p shares the highest degree of sequence identity (52.4%) with its human ortholog XRCC4 (Figure 1A). The overall identity between Lif1p and XRCC4 is ~20%. *Vice versa*, examination of different fragments of Ntr1p in two-hybrid

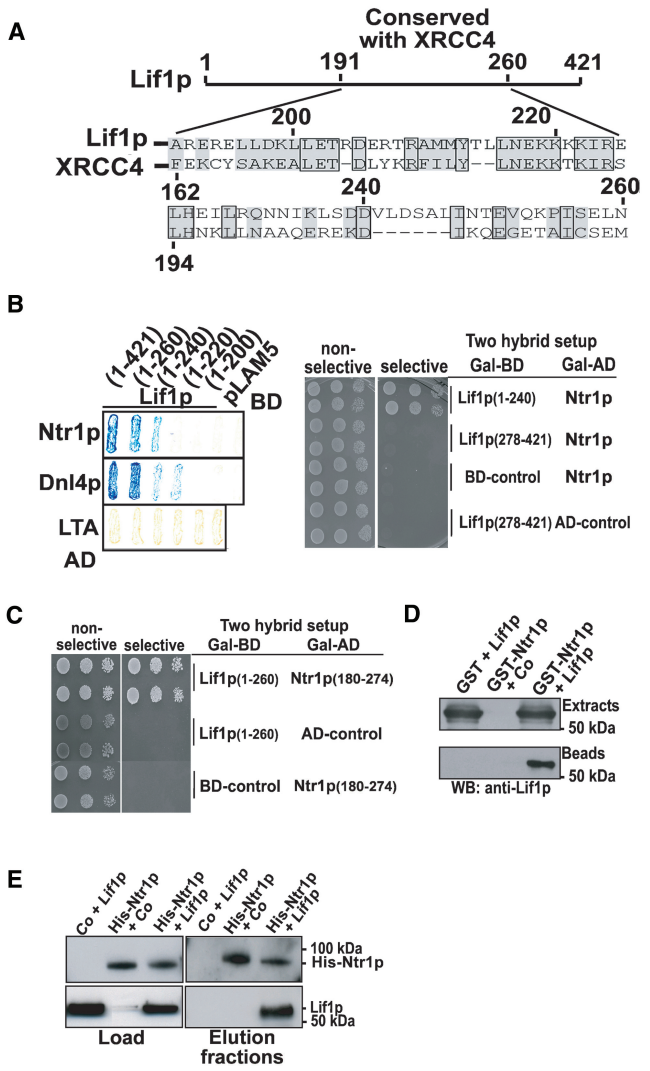

Figure 1. Ntr1p interacts with Lif1p. (**A**) Amino acid alignment of the conserved core region of *S. cerevisiae* Lif1p and human XRCC4. (**B**) Mapping of Ntr1p and Dnl4p interaction domains of Lif1p. Left panel: β-Galactosidase assays of yeast two-hybrid analyses; right panel: two-hybrid analyses with serial dilutions of two independent colonies plated on non-selective (-Leu-Trp) and selective (-Leu-Trp-His) media. Different fragments of Lif1p were expressed as BD (Gal4 DNA-binding domain) fusion proteins (numbers in brackets indicate amino acids). Gal4 activation domain (AD) constructs are fusions of the coding sequences for amino acids 89–509 of Ntr1p and the entire ORF of Dnl4p. LTA is SV40 large T-antigen, pLAM5 is human lamin C (66–230). (**C**) Mapping of Lif1p interaction domain of Ntr1p with the indicated fusion proteins of Lif1p and Ntr1p. Two-hybrid analyses were performed as described for the right panel of Figure 1B. (**D**) Copurification of Lif1p from bacteria expressing recombinant Lif1p and GST-fused Ntr1p. Western blot (WB) analysis of bacterial extracts and glutathione sepharose-bound proteins using anti-Lif1p antibody. Upper panel: 20 μg of extracts expressing Lif1p and GST-Ntr1p proteins as indicated. Lower panel: Lif1p copurification from 1 mg of soluble proteins after pull down of GST-tagged proteins and several washes at high salt stringency. Co indicates the vector control for Lif1p. Here, 5 μl out of 30 μl of proteins eluted from the beads were applied. (**E**) Copurification of Lif1p from *S. cerevisiae* expressing 6× histidine-fused Ntr1p (His-Ntr1). Co indicates the vector control. Proteins were co-expressed in yeast and histidine-fused proteins were purified using nickel agarose. Amounts of proteins used for affinity purification and WB analysis were the same as in (D). WB analysis of relevant elution fractions using anti-Lif1p or an antibody directed against 6× histidine (anti-His).

experiments located the Lif1p-interacting site between amino acids 180 and 274 of Ntr1p (Figures 1C and S1). This region of Ntr1p was previously shown to be involved in the interaction with Ntr2p, another spliceosome disassembly factor (17). Notably, several N-terminal truncations of Ntr1p that contained the Lif1p interaction domain and the entire C-terminus exhibited marked toxicity in the two-hybrid assay, some of them only under co-expression of Lif1p (data not shown).

We then applied GST- and Ni^{2+}-NTA-based fractionation techniques to corroborate the interaction between Ntr1p and Lif1p. Indeed, co-expression of Lif1p with GST-tagged (GST-Ntr1p) or 6-histidine-tagged Ntr1p (His-Ntr1p) in bacteria and in *S. cerevisiae*, respectively, allowed specific and efficient copurification of Lif1p with the tagged Ntr1p, and this after stringent washing with 637 mM NaCl, 0.2% NP40 and 20% glycerol (Figure 1D and E).

Ntr1p is a conserved G-patch protein

Homology searches identified Ntr1p orthologs in species across all eukaryotic kingdoms. A putative human ortholog (presently denominated as TFIP11 for tuftelin-interacting protein) shares an overall 22% identity and 40% similarity with the yeast Ntr1p (Figure S1). This homology stretches over the entire length of the protein and shows a degree of conservation that is also found in other yeast and human orthologs, including the NHEJ factors DNA ligase IV/Dnl4p or XRCC4/Lif1p (3,4,37). All orthologs are characterized by the presence of a more highly conserved N-terminal G-patch domain (Figure S1). For Ntr1p, it was shown that the G-patch is necessary for the interaction with Prp43, an RNA helicase associated with the spliceosome disassembly complex (17). Several G-patch-containing proteins have functions in DNA and RNA metabolism. One family member, PinX1, was recently shown to have dual functions in telomere maintenance (22,28,29) and in ribosomal and small nucleolar RNA maturation (30). Others, such as the *A. thaliana* DRT111 and *T. gondii* TgDRE were shown to have functions in DNA repair by complementing UV and mitomycin hypersensitivity of *E. coli ruvC* and *recG* mutant strains (21,23,24). *Drosophila melanogaster* SPF45 could partially complement MMS sensitivity of *E. coli recG* mutant strains, and mutant *spf45* mutant animals displayed an MMS-sensitive mutant phenotype (25).

Ntr1p is an essential protein

To examine the role of Ntr1p in NHEJ in yeast, we disrupted the *NTR1* gene by replacement of the entire YLR424W ORF with a marker gene cassette in a diploid wild-type background (4). Subsequent sporulation of the heterozygous *NTR1*/*ntr1*Δ to haploid progeny revealed a lethal phenotype of the *NTR1* disruption. Spores carrying the *ntr1*Δ allele were able to germinate but the resulting cells then arrested growth after two cell divisions with a large budded morphology (data not shown). This stands in clear contrast to the rather mild phenotype of a NHEJ defect in yeast and may be explained by the essential functions of Ntr1p in spliceosome disassembly (17–19).

Numerous attempts of generating conditional and separation of function mutants of NTR1 by directed and random mutagenesis, N-degron-tagging and metabolic depletion approaches failed, the lethal phenotype always dominated putative non-essential DSBR defects in all experiments. As regards human NTR1/TFIP11 (from now on referred to as NTR1 only), northern blot analysis of total cellular RNA from human fibroblasts confirmed that it is an active and ubiquitously expressed gene in fetal and adult tissues, producing a transcript of 2.9 kb, which is consistent with the largest cDNA sequence reported (DKFZp434B194) (Figure S2A).

Yeast Ntr1p and Dnl4p form mutually exclusive complexes with Lif1p and Nej1p

Given the proximity of the Dnl4p and Ntr1p interaction sites in the core domain of Lif1p, we examined the effect of Ntr1p on the formation of the DNA ligase complex, i.e. Dnl4p/Lif1p/Nej1p, of NHEJ using a three-hybrid approach. Nej1p, a cell-type-specific regulator of NHEJ was shown to interact with the N-terminus of Lif1p (15). In these experiments, the co-expression of Ntr1p significantly reduced the two-hybrid interaction between Lif1p and Dnl4p (Figure 2), while it had no effect on the interactions between p53 and SV40-LTA (data not shown) or Nej1p and Lif1p (Figure 2). Hence, in this assay Ntr1p interfered specifically with the formation of the Lif1p/Dnl4p complex. Furthermore, Nej1p binds the N-terminal region of Lif1p between amino acids 2 and 69 (15), but it does not interact directly with Dnl4p or Ntr1p in a two-hybrid experiment. However, co-expression of Lif1p mediates close proximity of Nej1p and Ntr1p (or Dnl4p, data not shown), thus allowing survival under selective conditions in a three-hybrid setup, and this is independent of whether Nej1p or Ntr1p are fused to the Gal-AD or the Gal-DB domain (Figure 2). Thus, Lif1p is able to act as a bridging factor for both proteins, indicating that, under three-hybrid conditions, Lif1p and Nej1p form two alternative ternary complexes, one that contains Dnl4p and another that contains Ntr1p.

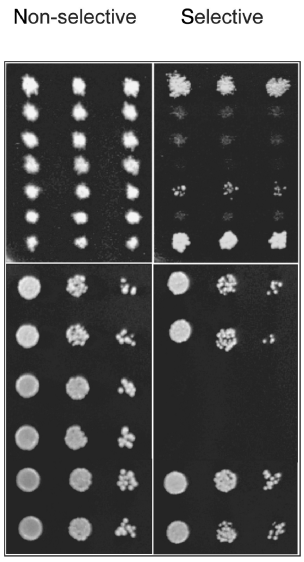

Three-hybrid setup		
Gal 4-BD	MET	Gal 4-AD
$Lif1p_N$	–	$Dnl4p_C$
$Lif1p_N$	Ntr1p	$Dnl4p_C$
$Lif1p_N$	Ntr1p	$Dnl4p_C$
$Lif1p_N$	–	AD-control
BD-control	–	$Dnl4p_C$
$Lif1p_N$	Ntr1p	AD-control
p53	–	SV40LTA
Nej1p	–	Lif1p
Nej1p	Ntr1p	Lif1p
Nej1p	–	Ntr1p
Ntr1p	–	Nej1p
Nej1p	Lif1p	Ntr1p
Ntr1p	Lif1p	Nej1p

Figure 2. Interference of Ntr1p with the formation of NHEJ-relevant protein complexes in yeast three-hybrid analyses. Full-length Nej1p, Ntr1p, Lif1p, or domains of Dnl4p ($Dnl4p_C$, amino acids 632–945), Lif1p ($Lif1p_N$, amino acids 1–260) were expressed as Gal4-BD or Gal4-AD fusions. Where indicated (MET), Ntr1p or Lif1p were expressed under the control of a methionine-repressible promotor. p53 and SV40LTA serve as positive controls for protein interactions. BD and AD are vector controls pBridge and pACT2, respectively. One representative colony out of four analyzed is plated as a serial dilution on appropriate selection media (non-selective, -Leu-Trp; selective, -Leu-Trp-His-Met) and grown for 4 days.

Overexpression of Ntr1p affects DNA DSBR efficiency in yeast

The negative effect of Ntr1p on the formation and/or stability of Dnl4p/Lif1p complexes (Figure 2) prompted us to examine a possible negative regulatory role of Ntr1p in NHEJ. First, we assessed the NHEJ efficiency of cells expressing endogenous levels or an excess Ntr1p in a plasmid re-ligation assay. This assay measures the relative efficiency of homology-independent joining of double-stranded DNA ends of a linearized plasmid upon transformation of yeast cells (4). We found that overexpression of different variants of NTR1 (full-length untagged and EGFP-tagged protein, Lif1p-interaction competent truncations) in wild-type cells and in the background of an EGFP-Ntr1p complemented *ntr1*Δ deletion strain consistently reduced plasmid ligation efficiency by 2–3-fold (Figures 3, S3 and data not shown). Suppression of NHEJ was apparent with both EcoRI and PstI cut plasmid, i.e. on substrates with 5′ and 3′ single-stranded overhangs, respectively (Figure 3A). Yet, the precision of the end-joining events was not affected as determined by PCR amplification and re-digestion of the junctions (data not shown). Co-expression of Lif1p restored plasmid rejoining efficiency to near wild-type levels (Figure S3). In a *dnl4*Δ deficient strain, however, overexpression of Ntr1p did not further reduce plasmid re-ligation efficiency. Thus, overexpression of Ntr1p reduces mildly but reproducibly and significantly Dnl4p-dependent plasmid re-circularization.

To address the role of Ntr1p in the repair of chromosomal DNA breaks, we tested the resistance of DSBR-proficient and -deficient yeast cells expressing endogenous levels or an excess of Ntr1p to DSBs generated by the endonucleases HO or EcoRI (34). Expression of HO in *S. cerevisiae* induces cleavage of the chromosomal DNA once at the *MAT* locus. The resulting DSB is repaired by *RAD52*-dependent HR, a process engaging an intact donor sequence from either of two silent mating-type loci (*HML* or *HMR*) located on the same chromosome (38). Unlike HO, EcoRI will often generate breaks at homologous positions in sister chromatids that require repair by NHEJ rather than by HR. We thus established strains carrying plasmid constructs for the expression of either of these nucleases under the control of the *GAL1* promoter, and of *NTR1* under the control of the constitutive *ADH1* promoter. Note that the *NTR1* construct used here produced an N-terminal GAL4-DNA-BD-fusion of Ntr1p, the functionality of which had been validated first by complementation of

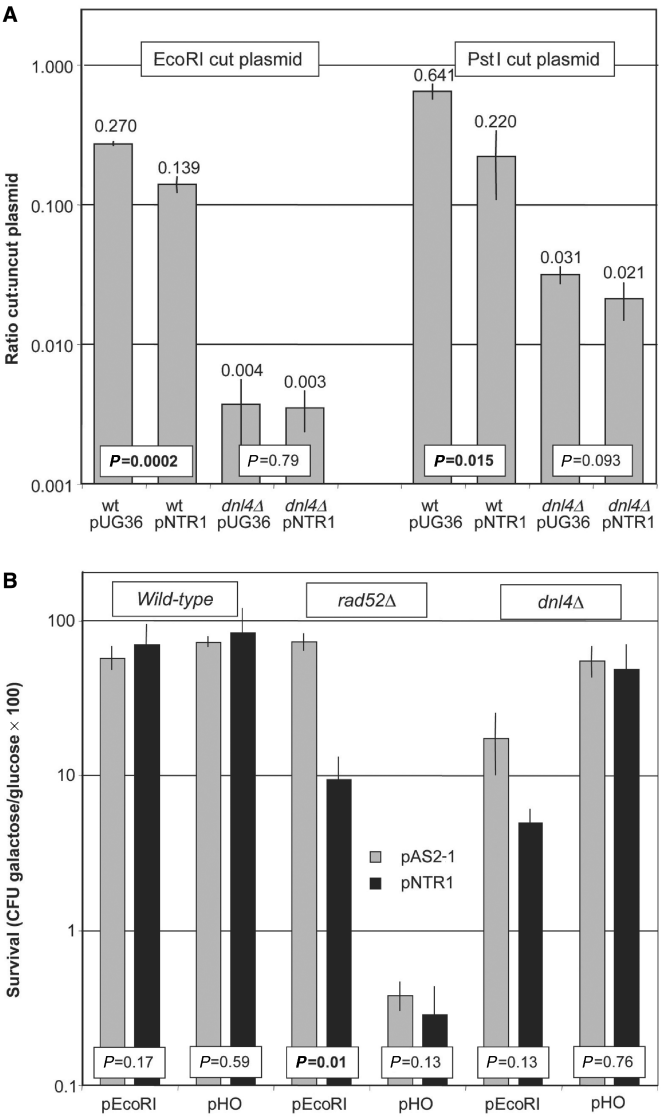

Figure 3. Ntr1p overabundance affects NHEJ of linearized plasmid DNA transformed into yeast, or of chromosomal DNA double-strand breaks in different genetic backgrounds. (**A**) Wild-type (wt) or NHEJ-deficient *dnl4*Δ yeast strains constitutively producing full-length EGFP-tagged-Ntr1p from plasmid pUG36 (vector control) were transformed with equal amounts of digested or undigested plasmid pBTM116, which is a substrate for NHEJ (4). Results are presented as relative transformation efficiencies (ratios of cut:uncut plasmid). EcoRI cut indicates 5′-overhangs, PstI cut indicates 3′-overhangs. Error bars represent one standard deviation, statistical significance (*P*-values) by a two-tailed students *t*-test is indicated. (**B**) Wild-type (wt), HR-deficient *rad52*Δ, or NHEJ-deficient *dnl4*Δ strains constitutively producing full-length Ntr1p from plasmid pAS2–1. Chromosomal breaks were induced by additional expression of EcoRI or HO (GAL1-inducible) upon transformation of the respective expression vectors (35). Results are presented as percentage of survival of cells carrying an NTR1-expressing vector or the respective control vector (pAS2-1) when grown on galactose containing medium. Error bars represent one standard deviation, *P*-values of a two-tailed students *t*-test are indicated.

the lethality of an *ntr1*Δ strain. Parental vector controls were included to assess Ntr1p-specificity of the effects following nuclease induction. Cells carrying these constructs were cultured in the presence of glucose and then dropped in serial dilutions onto media containing either glucose or raffinose/galactose.

Consistent with a predominance of the HR pathway in the repair of HO-induced DSBs, we found *rad52*Δ cells, but not *dnl4*Δ cells, to be highly sensitive to HO expression (survival: wild-type, 73%; *rad52*Δ, 0.38%). *Vice versa*, *dnl4*Δ cells were more sensitive to EcoRI-induced DSBs (survival: wild-type, 58%; *dnl4*Δ, 17%) than *rad52*Δ cells (Figure 3B). These results confirm that cells proficient in HR do rarely employ NHEJ to repair HO-induced DSBs at the MAT locus, and that breaks generated by EcoRI are dealt with predominantly by NHEJ. Ntr1p expression had little effect on the wild-type cells in this assay, but it clearly sensitized the *rad52*Δ (8-fold) and somewhat less the *dnl4*Δ (3.5-fold) mutant strains to DNA strand breaks generated by EcoRI. The suppression of the viability in the *rad52*Δ background is statistically significant, implicating that an excess of Ntr1p channels the repair of EcoRI-induced DSBs into the HR pathway, which, in this strain, is non-functional. Although a similar trend was notable in the *dnl4*Δ mutant, this effect is not statistically significant, suggesting that Ntr1p does not interfere with DSBR in an NHEJ-deficient, HR-proficient background. Consistently, Ntr1p overexpression had little effect on cellular survival upon inductions of HO breaks, which are predominantly repaired by the HR pathway. Thus, Ntr1p affects plasmid ligation efficiency and the productive repair of chromosomal EcoRI breaks by NHEJ.

Human NTR1 is a structural and functional homolog of yeast Ntr1p

Although the evolutionary conservation of the Ntr1p seems clear, much of it appears to be accounted for by the presence of the G-patch. The interaction of Ntr1p with Lif1p, however, requires less conserved sequences downstream of the G-patch (Figure S1). We wondered whether this interaction is conserved in humans and thus examined if human NTR1 forms a complex with XRCC4, the human ortholog of yeast Lif1p. Following deletion of N- and C-terminal sequences of NTR1, which was necessary to reduce autoactivation in two-hybrid assays, we were able to show a specific interaction between XRCC4 and NTR1 (Figure 4A). Like for the yeast counterparts, we could confirm this interaction in a GST-copurification experiment with GST-tagged NTR1 and XRCC4 co-expressed in *E. coli* (Figure 4B). Using this assay, we also mapped the XRCC4 interaction region within NTR1 to amino acids 289 – 343 (Figures 4B, S1), which coincides with the Lif1p interaction domain of yeast Ntr1p (Figure S1). In addition, glutathione sepharose beads coated with bacterially expressed GST-NTR1 (192–580) were able to recover endogenous human XRCC4 protein from HeLa cell extracts (Figure 4C). Further evidence for structural homology between the yeast and human NTR1 proteins came from experiments with antisera raised against the two proteins. Both antisera showed cross-reactivity with the respective orthologous NTR1 proteins, despite the fact that the antibody against the human

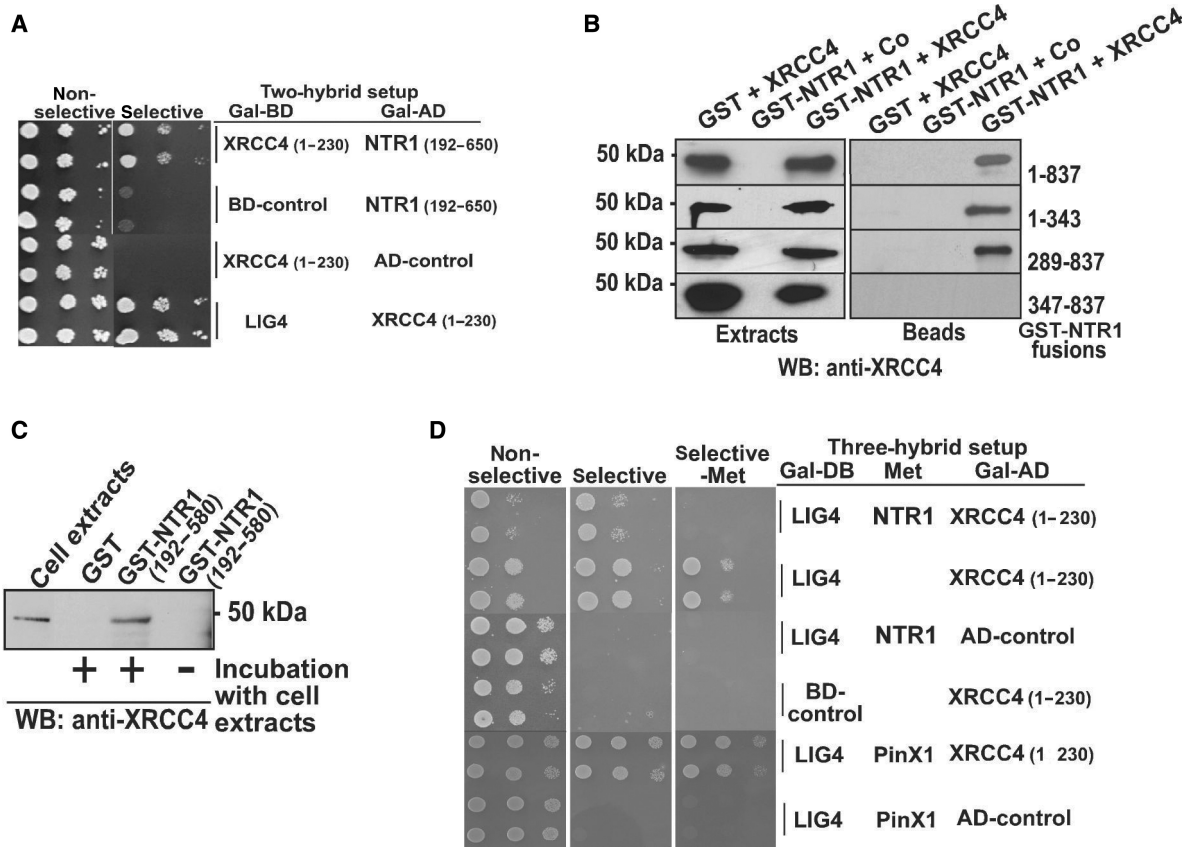

Figure 4. Human NTR1 interacts with XRCC4. (**A**) Two-hybrid interaction of huNTR1 and XRCC4. Fragments containing the indicated amino acids of XRCC4 (1–230), NTR1 (192–650) and full-length LIG4 were fused to the Gal4 DNA-binding (Gal-DB) and activation domains (Gal-AD) as indicated. Serial dilutions of two randomly picked clones were plated on appropriate selection media (as in Figure 1B). (**B**) Copurification of XRCC4 from bacteria expressing recombinant XRCC4 and various fragments of GST-tagged huNTR1. Western blot analysis of bacterial extracts and glutathione sepharose-bound proteins using anti-XRCC4 antibody (experimental conditions as in Figure 1D). The upper panel shows expression of recombinant XRCC4 in 20 μg of bacterial extracts in different combinations with a GST-expressing vector or GST-fused NTR1. The lower panel shows XRCC4 copurification after pull down of GST-fused full-length and truncated forms of NTR1 (amino acids as indicated). (**C**) Purification of XRCC4 from HeLa cell extracts with GST-NTR1 (192–580)-coated glutathione sepharose beads. GST-NTR1 or GST-containing beads were incubated HeLa cell extracts overnight and stringently washed. Western blot analysis of eluted proteins was performed with anti-XRCC4. (**D**) Overexpression of NTR1 disrupts interaction between LIG4 and XRCC4 in three-hybrid analyses. LIG4 and XRCC4 (1–230) were fused to the Gal4-BD and -AD, respectively. NTR1 and PinX1 (used as control) were expressed under the control of a methionine-repressible promotor where indicated. Serial dilutions of two randomly picked clones. Experimental conditions as in Figure 2.

NTR1 was raised against a fragment (289–837) that lacked the conserved G-patch (Figure S2B).

Functionally, three-hybrid experiments with human LIG4, NTR1 and XRCC4 showed that, like its yeast counterpart, human NTR1 interferes with two-hybrid interaction between LIG4 and XRCC4, suggesting that NTR1 competes with LIG4 for the binding site in XRCC4 (Figure 4D). However, while we were successful in co-immunoprecipitating endogenous DNA ligase IV (or Dnl4p) with XRCC4 (or Lif1p), we have thus far not been able to do the same for the endogenous NTR1 proteins (data not shown). The interaction between NTR1 and XRCC4 (or Lif1p) may be short-lived and/or occurs only under specific physiological conditions, e.g. in particular phases of the cell cycle and/or in response to certain forms of genotoxic stress.

Despite the structural and functional conservation between the yeast and the human NTR1 proteins, however, expression of human NTR1 in yeast failed to rescue the lethality of an *ntr1*Δ mutation (data not shown).

Human and yeast NTR1 interact with PinX1, another G-patch protein

To get further clues regarding the function of NTR1, we performed two-hybrid screening of a HeLa cDNA library with a fragment of human NTR1 (1–580). This identified PinX1 as an additional interaction partner. Mapping of the PinX1 interaction domain of NTR1 located the contact site between amino acids 192 and 580 (Figure 5A). This is C-terminal to the conserved G-patch and overlaps with the region required for interaction with XRCC4 (289–343). In addition, co-expression of NTR1 with GST-tagged PinX1 (GST-PinX1) bacteria allowed specific and efficient copurification of NTR1 with the tagged PinX1 (Figure 5B), and glutathione sepharose beads coated with bacterially expressed GST-NTR1 (192–580) were able to recover

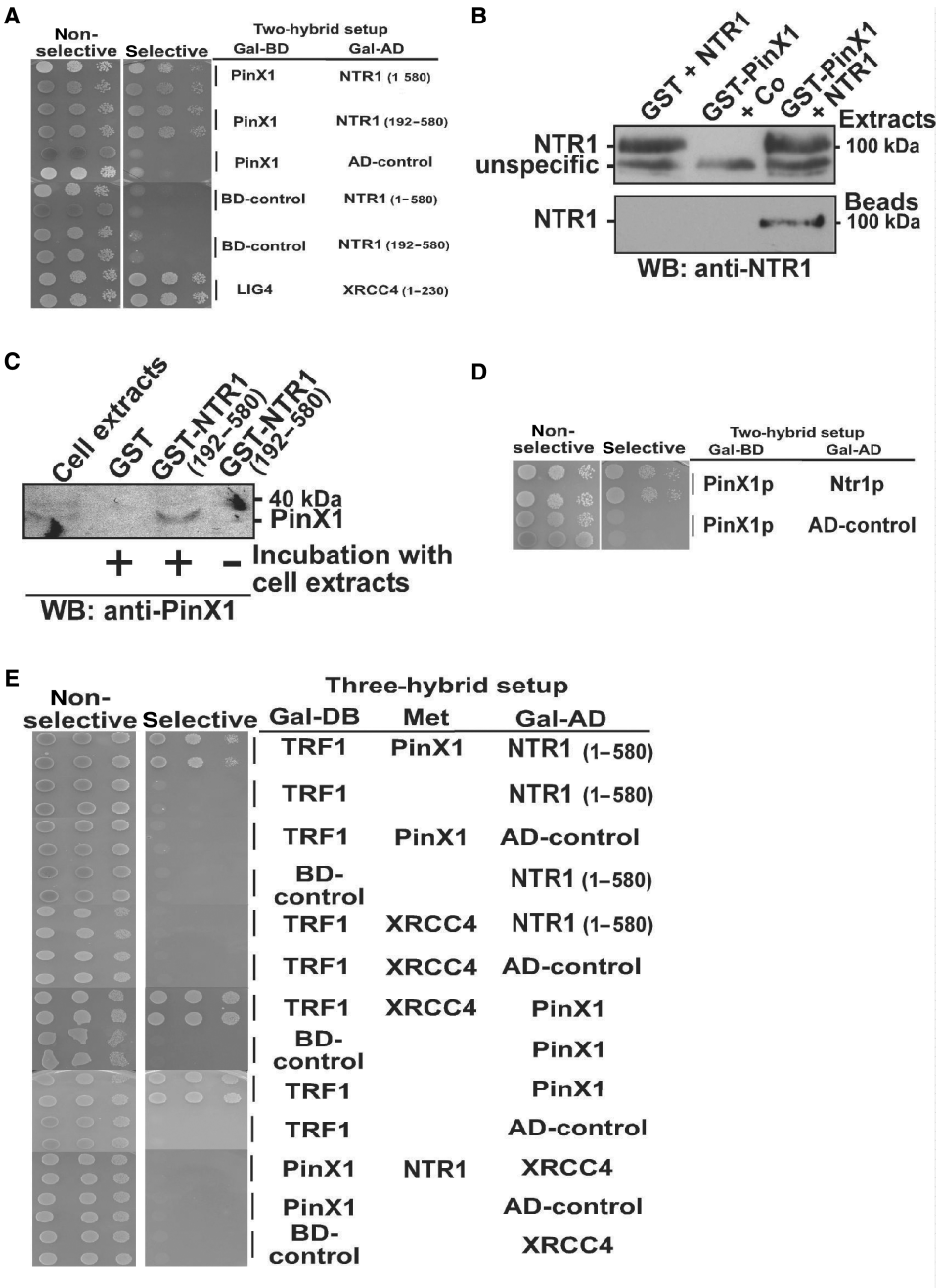

Figure 5. Yeast and human NTR1 interact with the respective orthologs of PinX1. (**A**) Two-hybrid interaction of human NTR1 and PinX1. Two-hybrid analyses were performed with the indicated Gal-BD and -AD fusions of PinX1 and NTR1. Numbers in brackets indicate amino acids. Experimental conditions as in Figure 1B. The interaction of LIG4 and XRCC4 (1–230) was used as a positive control. (**B**) Copurification of human NTR1 from bacteria expressing recombinant NTR1 and GST-fused PinX1. Experimental conditions as in Figure 1D. western blot (WB) analysis of bacterial extracts and glutathione sepharose-bound proteins using anti-NTR1 antibody. Upper panel: expression of recombinant NTR1 in 20 µg of bacterial extracts in the presence of a GST-expressing vector (GST) and a vector expressing a GST-fused form of PinX1 (GST-PinX1). Lower panel: corresponding NTR1 copurification after pull down of GST-tagged proteins and several washes at high salt stringency. (**C**) Purification of PinX1 from HeLa cell extracts with GST-NTR1 (192–580). Experimental conditions as in Figure 4C. Western blot analysis was performed with anti-PinX1. (**D**) Two-hybrid interactions of yeast Ntr1p and PinX1p. Experimental conditions as in Figure 1B. (**E**) Overexpression of PinX1 mediates proximity between NTR1 and TRF1 in three-hybrid analyses. Serial dilutions of two randomly picked clones. Experimental conditions as in Figure 2. TRF1 and NTR1 (1–580) were fused to the Gal4-BD and -AD, respectively. PinX1, XRCC4 or NTR1 were expressed under the control of a methionine-repressible promotor whereever indicated.

endogenous human PinX1 protein from HeLa cell extracts (Figure 5C). Again, this interaction appears to be conserved between yeast and human, as PinX1p figures in the list of the many interaction partners of Ntr1p previously identified in genome wide two-hybrid screens for protein-protein interactions (39) and could be reproduced in an additional two-hybrid analysis of the yeast proteins (Figure 5D).

Human PinX1 was first identified as an interaction partner of the telomere-binding protein Pin2/TRF1 and subsequently shown to regulate telomerase activity (22,29). The yeast PinX1p has been associated with rRNA and nucleolar RNA maturation (30) as well as to interact physically with telomerase to regulate its catalytic activity (28). Hence, the link to PinX1 suggested a function of NTR1 at telomeres. We therefore asked whether human PinX1 might act as a bridging factor between NTR1 and TRF1. Indeed, co-expression of PinX1 mediated close proximity of NTR1 and TRF1, allowing cells to grow under selective conditions in the three-hybrid assay (Figure 5E). Thus, TRF1 and NTR1 bind PinX1 simultaneously, which may provide a structural link of NTR1 to telomere metabolism.

Human and yeast NTR1 co-localize with telomere-associated proteins

To corroborate an association of NTR1 with telomeres, we used confocal microscopy and live cell imaging to localize the protein in cells. Expression of a functional EGFP-Ntr1p under the control of the inducible MET25 promoter in NTR1-proficient and -deficient (*ntr1*Δ) yeast cells revealed a nuclear localization of the protein with a dot-like pattern (Figure 6A). These dots varied in numbers and intensity depending on the expression level and the cell ploidy (data not shown). We thus performed co-localization studies under repressed conditions and in haploid cells, where the EGFP-Ntr1p protein level approximates that of the endogenous protein and NHEJ is active (data not shown). We found significant co-localization of the EGFP-Ntr1p dots with endogenous Rap1p, a transcriptional regulator that binds to telomeric sequences and contributes to telomere maintenance and the establishment of the telomere position effect on gene expression (40). Here, $63 \pm 2\%$ (165/262 observations, three independent experiments) of double-positive cells showed complete or partial (>30% of signal) overlap of all EGFP-Ntr1 and Rap1p signals, $14 \pm 2\%$ of cells showed both, co-localizing and separate Ntr1p and Rap1p foci, whereas $24 \pm 1\%$ of cells showed no co-localization of the two proteins (Figure 6A). Thus, the fraction of cells showing co-localization of EGFP-Ntr1p with Rap1p was significantly higher than that without co-localization ($P = 0.0001$, *t*-test). Nevertheless, prompted by the incompleteness of the co-localization with Rap1p and the localization properties of PinX1, which is found not only at telomeres but also in the nucleolus (22), we tested whether Ntr1p might behave similarly. Hence, we examined co-localization of Ntr1p with Nop1p, a nucleolar protein involved in rRNA processing (41). Indeed, we found EGFP-Ntr1p foci to overlap with the signal of a CFP-tagged Nop1p in 74% (118/159 observations, two independent experiments) of the cells, suggesting a possible association of Ntr1p with the nucleolus (Figure 6A). Interestingly, telomeric and nucleolar localization has been described for a number of telomere-associating proteins, including the reverse transcriptase subunit of the telomerase itself (42).

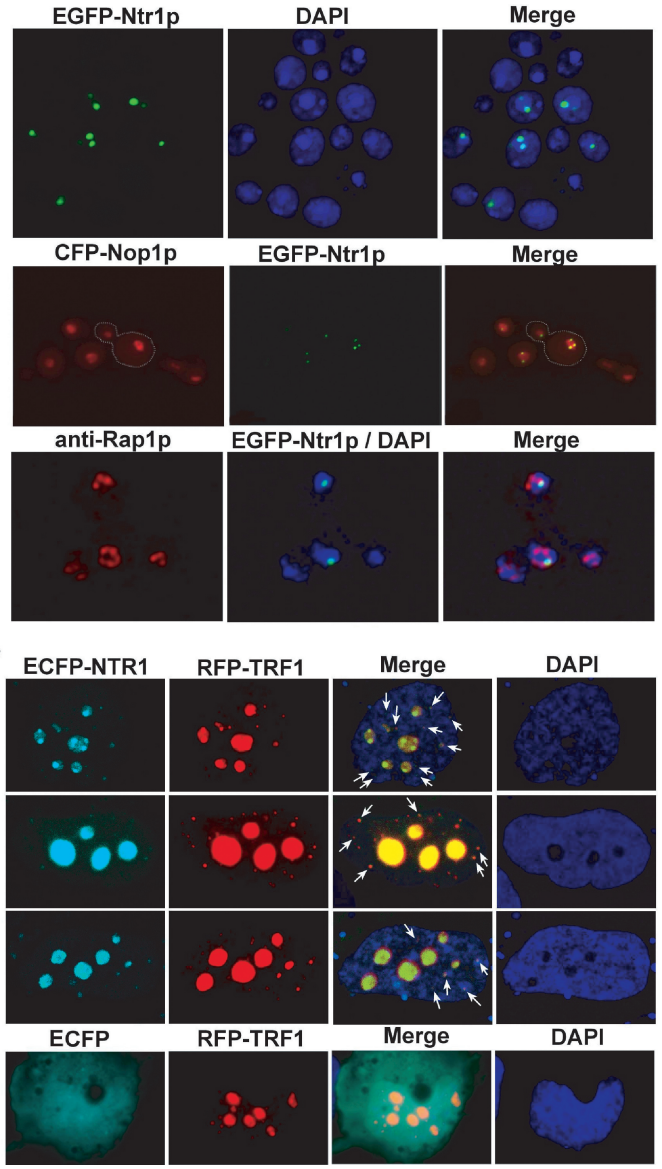

Figure 6. Yeast and human NTR1 co-localize with nucleolus- and telomere-associated proteins. (**A**) Intracellular localization of Ntr1p and co-localization with other proteins. Upper panel: EGFP-Ntr1p (green) localizes to the nucleus (DAPI, light blue) and forms foci. Middle panel: live cell images of CFP-Nop1p (red, false color) and EGFP-Ntr1p (green). Co-localizing signals are shown in yellow in the merge panel. Lower panel: confocal images of EGFP-Ntr1p (green) in fixed cells immunostained for Rap1p (red). DAPI staining of DNA is shown in blue. Co-localization between the two proteins is shown in yellow on the merge panel. (**B**) Intracellular localization of human NTR1 and TRF1. WI26 VA4 cells were co-transfected with expression constructs of ECFP-NTR1 (amino acids 289–580) and RFP-TRF1 (upper three panels). eCFP was used as a control (lower panel). Co-localization in confocal images is shown in yellow on the merge panel and telomeric co-localization is indicated by arrows.

Overexpression of full-length NTR1 in human cell lines was toxic and resulted in aggregate formation and cell lysis. To analyze intracellular localization of human NTR1, we therefore expressed a non-toxic ECFP-NTR1 fragment that contained the interaction region with XRCC4 and PinX1. Upon co-transfection of

ECFP-NTR1 and RFP-TRF1 expressing constructs, we found a nucleolar co-localization in all double-transfected cells. The double-transfected cells showed 40% full and 44% partial co-localization of extranucleolar ECFP-NTR1 foci with RFP-TRF1, indicating an association of NTR1 with telomeres (Figure 6B). A similar telomeric and nucleolar co-localization pattern was previously described for PinX1 and TRF1 (22).

Together, these data support a link between NTR1 function and telomere metabolism as suggested by the three-hybrid interaction observed between NTR1, PinX1 and TRF1.

DISCUSSION

This work establishes a specific physical interaction of the yeast Lif1p and Ntr1p proteins. Ntr1p is G-patch-motif-containing protein that has recently been described to function in spliceosome disassembly. It interacts with Lif1p through its Dnl4p-binding site and, in doing so, forms a complex with Lif1p-Nej1p that lacks the catalytic DNA ligase function. This would implicate a role of Ntr1p in the regulation of NHEJ by sequestering the DNA ligase cofactor Lif1p in an inactive complex. Consistently, overproduction of Ntr1p in yeast cells affects the efficiency of joining of linearized plasmids and alters the way cells process chromosomal DSBs by NHEJ. Ntr1p itself as well as its interaction with the DNA ligase IV cofactor has been conserved in evolution; we show that the human ortholog NTR1 interacts with XRCC4 in a way that excludes the LIG4 in the complex. An additional conserved interaction of the yeast and human NTR1 proteins with PinX1, a G-patch protein implicated in nucleolar RNA maturation and regulation of telomerase activity, and their localization to telomeres and the nucleolus suggests an additional function of the splicing factor in location-dependent regulation of NHEJ.

Consistent with its physical interactions (39), recently published work strongly suggests that the essential function of Ntr1p is the processing/maturation of RNA (17–19). Still, as telomeric terminal rearrangements in yeast and human cells are know to be generated by NHEJ and, thus, to depend on functional DNA ligase IV (43,44), we wanted to exclude that uncontrolled fusion of telomeres contributes to the lethal phenotype of the *ntr1*Δ mutant, i.e. that the loss of Ntr1p leads to a de-repression of fatal ligation of free telomere ends. We therefore tested whether the lethality of the *ntr1*Δ mutation can be rescued by an additional *dnl4*Δ or *lif1*Δ defect. This was not the case, indicating that aberrant Dnl4p-mediated ligation of double-stranded DNA ends is not a dominant killing event in the *ntr1*Δ strains. Various attempts to generate NTR1 variants that separate the essential splicing function from the DNA repair function failed. In retrospect, however, this may not be too surprising, considering that the sites for Lif1p and Ntr2p interactions map to the same region of Ntr1p (17). Thus, the role of NTR1 in NHEJ is difficult to address in an unambiguous genetic approach and therefore remains somewhat enigmatic. While there is no evidence for a Dnl4p-independent function of Lif1p (or XRCC4), our plasmid ligation and nuclease survival experiments implicate that Ntr1p, when present in excess, affects the cellular DSBR capacity. The effects, however, though reproducible and statistically significant, are complex and difficult to interpret. In the plasmid ligation assay, overexpression of *NTR1* inhibits NHEJ in a Dnl4p-dependent manner. Yet, compared to a full NHEJ deficiency, this effect is only marginal. In the chromosomal DSBR assay, NTR1 overexpression sensitizes *rad52*Δ cells to EcoRI-induced DSBs to the level of a *dnl4*Δ single mutant, but it remains to be clarified why this effect requires *RAD52* to be inactive. One explanation is that excess Ntr1p and the loss of Dnl4p affect NHEJ at different intermediate stages of the process, the former allowing more efficient rescue of the repair event by the HR pathway and the latter leading to more frequent unproductive (lethal) processing of the EcoRI breaks. An important caveat associated with the interpretation of these results is that the assays used may not adequately mimic the relevant physiological environment for Ntr1p action.

Indeed, the subnuclear localization of Ntr1p as well as its interaction with PinX1 suggests that it acts locally rather than globally in the genome. EGFP-tagged Ntr1p expressed at about endogenous levels from a repressed MET25 promoter localizes to one to two, rarely three, distinct foci in the nucleus. Statistical analyses of these co-localization experiments suggest that, one of these spots seems to non-randomly associate with the nucleolar region (45), while the other(s) may reflect variable associations with telomeres. Interestingly, nucleolar and telomeric localization was also proposed for yeast and human PinX1, which we show here to interact with the respective NTR1 proteins. Besides its role in rRNA and nucleolar RNA maturation (30), yeast PinX1p was recently reported to regulate telomerase by sequestering its catalytic subunit in an inactive complex, presumably in the nucleolus (28). A similar regulatory mechanism could apply to the inhibition of NHEJ by Ntr1p. Ntr1p may sequester Lif1p and thereby prevent the formation or in fact mediate the disassembly of active DNA ligase complexes. Since this will occur only at sites where Ntr1p is enriched, presumably in the nucleolus or at the telomeres, the consequence will be a local inhibition of the ligation step of NHEJ. Testable predictions of such a scenario would be that Ntr1p localization is independent of Lif1p, while Lif1p should partially co-localize with Ntr1p in the nucleus. The focal Ntr1p localization pattern is indeed unaffected in a *lif1*Δ strain fulfilling the first prediction (data not shown). The Lif1p-Ntr1p co-localization, however, has not yet been resolved conclusively. The difficulty here is the diffuse nature of the nuclear localization of Lif1p, which may cover temporary or localized associations of the protein with alternative complexes. However, the localization of the spliceosome disassembly factor Ntr1p to telomeres and nucleoli and its interaction with Lif1p implicate unexpected functions of this protein in telomere metabolism and possibly DNA repair. We do not know whether or not there is a common denominator between spliceosome disassembly and the functions implicated here. It is worth

noting, however, that Ntr1p-depleted cells accumulate lariat-introns as RNA-splicing intermediates, a structure that remotely reminds us of the telomeric loops.

It is unclear to date exactly how cells discriminate between chromosomal DSBs that need to be repaired and the double-stranded DNA ends at telomeres that must not be ligated. This discrimination, however, is likely to occur at the ligation step because upstream key factors of NHEJ, e.g. the Ku heterodimer and the MRE11/RAD50/NBS1, associate with both types of DNA ends. This is where the NTR1 proteins could come into play. Their physical and functional properties as described in this work make them likely candidates for the regulation of NHEJ at the intersection of DNA DSBR and telomere end protection, although the underlying mechanistic details remain to be elucidated.

ACKNOWLEDGEMENTS

We thank Dr Francis Fabre for yeast strains, Dr Susan Gasser for reagents and technical support, and Dr Lukas Landmann and Dr Iakowos Karakesisoglou for competent assistance in confocal microscopy. Preliminary experiments were performed by G.H. and P.S. at the Clare Hall Laboratories, South Mimms, UK and we thank Dr Tomas Lindahl for his interest and support. G.H. was supported by grant He 2675/2–3, 'Sonderforschungsbereich' SFB 589 from the 'Deutsche Forschungsgemeinschaft (DFG)' and by the Köln Fortune Program/Faculty of Medicine, University of Cologne. J.H. was supported by the Köln Fortune Program/Faculty of Medicine, University of Cologne and K.S.-H. by a short-term EMBO Fellowship. S.K. and P.S. were supported by the 'Bonizzi-Theler Stiftung', Zürich. Funding to pay the Open Access publication charge was provided by the DFG.

Conflict of interest statement. None declared.

REFERENCES

1. Ferreira,M.G. and Cooper,J.P. (2004) Two modes of DNA double-strand break repair are reciprocally regulated through the fission yeast cell cycle. *Genes Dev.*, **18**, 2249–2254.
2. Guirouilh-Barbat,J., Huck,S., Bertrand,P., Pirzio,L., Desmaze,C., Sabatier,L. and Lopez,B.S. (2004) Impact of the KU80 pathway on NHEJ-induced genome rearrangements in mammalian cells. *Mol. Cell*, **14**, 611–623.
3. Herrmann,G., Lindahl,T. and Schär,P. (1998) *Saccharomyces cerevisiae* LIF1: a function involved in DNA double-strand break repair related to mammalian XRCC4. *EMBO J.*, **17**, 4188–4198.
4. Schär,P., Herrmann,G., Daly,G. and Lindahl,T. (1997) A newly identified DNA ligase of *Saccharomyces cerevisiae* involved in *RAD52*-independent repair of DNA double-strand breaks. *Genes Dev.*, **11**, 1912–1924.
5. Teo,S.H. and Jackson,S.P. (1997) Identification of *Saccharomyces cerevisiae* DNA ligase IV: involvement in DNA double-strand break repair. *EMBO J.*, **16**, 4788–4795.
6. Wilson,T.E., Grawunder,U. and Lieber,M.R. (1997) Yeast DNA ligase IV mediates non-homologous DNA end joining. *Nature*, **388**, 495–498.
7. Teo,S.H. and Jackson,S.P. (2000) Lif1p targets the DNA ligase Lig4p to sites of DNA double-strand breaks. *Curr. Biol.*, **10**, 165–168.
8. Calsou,P., Delteil,C., Frit,P., Drouet,J. and Salles,B. (2003) Coordinated assembly of Ku and p460 subunits of the DNA-dependent protein kinase on DNA ends is necessary for XRCC4-ligase IV recruitment. *J. Mol. Biol.*, **326**, 93–103.
9. Collis,S.J., DeWeese,T.L., Jeggo,P.A. and Parker,A.R. (2005) The life and death of DNA-PK. *Oncogene*, **24**, 949–961.
10. Dudasova,Z., Dudas,A. and Chovanec,M. (2004) Non-homologous end-joining factors of Saccharomyces cerevisiae. *FEMS Microbiol. Rev.*, **28**, 581–601.
11. Williams,B. and Lustig,A.J. (2003) The paradoxical relationship between NHEJ and telomeric fusion. *Mol. Cell*, **11**, 1125–1126.
12. Riha,K., Heackock,M.L. and Shippen,D.E. (2006) The role of the nonhomologous end-joining DNA double-strand break repair pathway in telomere biology. *Annu. Rev. Genet.*, **40**, 237–277.
13. Frank-Vaillant,M. and Marcand,S. (2001) NHEJ regulation by mating type is exercised through a novel protein, Lif2p, essential to the ligase IV pathway. *Genes Dev.*, **15**, 3005–3012.
14. Kegel,A., Sjostrand,J.O. and Astrom,S.U. (2001) Nej1p, a cell type-specific regulator of nonhomologous end joining in yeast. *Curr. Biol.*, **11**, 1611–1617.
15. Ooi,S.L., Shoemaker,D.D. and Boeke,J.D. (2001) A DNA microarray-based genetic screen for nonhomologous end-joining mutants in Saccharomyces cerevisiae. *Science*, **294**, 2552–2556.
16. Valencia,M., Bentele,M., Vaze,M.B., Herrmann,G., Kraus,E., Lee,S.E., Schär,P. and Haber,J.E. (2001) NEJ1 controls non-homologous end joining in Saccharomyces cerevisiae. *Nature*, **414**, 666–669.
17. Tsai,R.T., Fu,R.H., Yeh,F.L., Tseng,C.K., Lin,Y.C., Huang,Y.H. and Cheng,S.C. (2005) Spliceosome disassembly catalyzed by Prp43 and its associated components Ntr1 and Ntr2. *Genes Dev.*, **19**, 2991–3003.
18. Boon,K.L., Auchynnikava,T., Edwalds-Gilbert,G., Barrass,J.D., Droop,A.P., Dez,C. and Beggs,J.D. (2006) Yeast ntr1/spp382 mediates prp43 function in postspliceosomes. *Mol. Cell. Biol.*, **26**, 6016–6023.
19. Pandit,S., Lynn,B. and Rymond,B.C. (2006) Inhibition of a spliceosome turnover pathway suppresses splicing defects. *Proc. Natl. Acad. Sci. USA*, **103**, 13700–13705.
20. Aravind,L. and Koonin,E.V. (1999) G-patch: a new conserved domain in eukaryotic RNA-processing proteins and type D retroviral polyproteins. *Trends Biochem. Sci.*, **24**, 342–344.
21. Pang,Q., Hays,J.B. and Rajagopal,I. (1993) Two cDNAs from the plant Arabidopsis thaliana that partially restore recombination proficiency and DNA-damage resistance to E. coli mutants lacking recombination-intermediate-resolution activities. *Nucleic Acids Res.*, **21**, 1647–1653.
22. Zhou,X.Z. and Lu,K.P. (2001) The Pin2/TRF1-interacting protein PinX1 is a potent telomerase inhibitor. *Cell*, **107**, 347–359.
23. Dendouga,N., Callebaut,I. and Tomavo,S. (2002) A novel DNA repair enzyme containing RNA recognition, G-patch and specific splicing factor 45-like motifs in the protozoan parasite Toxoplasma gondii. *Eur. J. Biochem.*, **269**, 3393–3401.
24. Frenal,K., Callebaut,I., Wecker,K., Prochnicka-Chalufour,A., Dendouga,N., Zinn-Justin,S., Delepierre,M., Tomavo,S. and Wolff,N. (2006) Structural and functional characterization of the TgDRE multidomain protein, a DNA repair enzyme from Toxoplasma gondii. *Biochemistry*, **45**, 4867–4874.
25. Chaouki,A.S. and Salz,H.K. (2006) *Drosophila* SPF45: a bifunctional protein with roles in both splicing and DNA repair. *PLoS Genet*, **2**, e178.
26. Zhou,Z., Licklider,L.J., Gygi,S.P. and Reed,R. (2002) Comprehensive proteomic analysis of the human spliceosome. *Nature*, **419**, 182–185.
27. Wen,X., Lei,Y.P., Zhou,Y.L., Okamoto,C.T., Snead,M.L. and Paine,M.L. (2005) Structural organization and cellular localization of tuftelin-interacting protein 11 (TFIP11). *Cell. Mol. Life Sci.*, **62**, 1038–1046.
28. Lin,J. and Blackburn,E.H. (2004) Nucleolar protein PinX1p regulates telomerase by sequestering its protein catalytic subunit in an inactive complex lacking telomerase RNA. *Genes Dev.*, **18**, 387–396.
29. Banik,S.S. and Counter,C.M. (2004) Characterization of interactions between PinX1 and human telomerase subunits hTERT and hTR. *J. Biol. Chem.*, **279**, 51745–51748.

30. Guglielmi,B. and Werner,M. (2002) The yeast homolog of human PinX1 is involved in rRNA and small nucleolar RNA maturation, not in telomere elongation inhibition. *J. Biol. Chem.*, **277**, 35712–35719.
31. Critchlow,S.E., Bowater,R.P. and Jackson,S.P. (1997) Mammalian DNA double-strand break repair protein XRCC4 interacts with DNA ligase IV. *Curr. Biol.*, **7**, 588–598.
32. Tirode,F., Malaguti,C., Romero,F., Attar,R., Camonis,J. and Egly,J.M. (1997) A conditionally expressed third partner stabilizes or prevents the formation of a transcriptional activator in a three-hybrid system. *J. Biol. Chem.*, **272**, 22995–22999.
33. Transy,C. and Legrain,P. (1995) The two-hybrid: an in vivo protein-protein interaction assay. *Mol. Biol. Rep.*, **21**, 119–127.
34. Schär,P., Fasi,M. and Jessberger,R. (2004) SMC1 coordinates DNA double-strand break repair pathways. *Nucleic Acids Res.*, **32**, 3921–3929.
35. Barnes,G. and Rio,D. (1997) DNA double strand break sensitivity, DNA replication, and cell cycle arrest phenotypes of Ku-deficient *Saccharomyces cerevisiae*. *Proc. Natl. Acad. Sci. USA*, **94**, 867–872.
36. Gotta,M., Laroche,T. and Gasser,S.M. (1999) Analysis of nuclear organization in Saccharomyces cerevisiae. *Methods Enzymol.*, **304**, 663–672.
37. Tugendreich,S., Bassett,D.E.Jr., McKusick,V.A., Boguski,M.S. and Hieter,P. (1994) Genes conserved in yeast and humans. *Hum. Mol. Genet. Spec. No.*, **3**, 1509–1517.
38. Haber,J.E. (1992) Mating-type gene switching in *Saccharomyces cerevisiae*. *Trends Genet.*, **8**, 446–452.
39. Hazbun,T.R., Malmstrom,L., Anderson,S., Graczyk,B.J., Fox,B., Riffle,M., Sundin,B.A., Aranda,J.D., McDonald,W.H. *et al.* (2003) Assigning function to yeast proteins by integration of technologies. *Mol. Cell*, **12**, 1353–1365.
40. Gotta,M., Laroche,T., Formenton,A., Maillet,L., Scherthan,H. and Gasser,S.M. (1996) The clustering of telomeres and colocalization with Rap1, Sir3, and Sir4 proteins in wild-type Saccharomyces cerevisiae. *J. Cell Biol.*, **134**, 1349–1363.
41. Tollervey,D., Lehtonen,H., Carmo-Fonseca,M. and Hurt,E.C. (1991) The small nucleolar protein NOP1 (fibrillarin) is required for pre-rRNA processing in yeast. *EMBO J.*, **10**, 573–583.
42. Teixeira,M.T., Forstemann,K., Gasser,S.M. and Lingner,J. (2002) Intracellular trafficking of yeast telomerase components. *EMBO Rep.*, **3**, 652–659.
43. Liti,G. and Louis,E.J. (2003) NEJ1 prevents NHEJ-dependent telomere fusions in yeast without telomerase. *Mol. Cell*, **11**, 1373–1378.
44. Smogorzewska,A., Karlseder,J., Holtgreve-Grez,H., Jauch,A. and de Lange,T. (2002) DNA ligase IV-dependent NHEJ of deprotected mammalian telomeres in G1 and G2. *Curr. Biol.*, **12**, 1635–1644.
45. Bystricky,K., Laroche,T., van Houwe,G., Blaszczyk,M. and Gasser,S.M. (2005) Chromosome looping in yeast: telomere pairing and coordinated movement reflect anchoring efficiency and territorial organization. *J. Cell Biol.*, **168**, 375–387.